Comparison of Hall Thruster Ion Dynamics Between Laser Induced Fluorescence Measurements and a 2-D Hybrid Simulation

IEPC-2015-438p／ISTS-2015-b-438p

Presented at Joint Conference of 30th International Symposium on Space Technology and Science,
34th International Electric Propulsion Conference and 6th Nano-satellite Symposium
Hyogo-Kobe, Japan
July 4–10, 2015

Christopher V. Young* and Eunsun Cha†
Stanford Plasma Physics Laboratory, Stanford, CA, 94305, USA

Eduardo Fernandez‡
Eckerd College, St. Petersburg, FL, 33711, USA

and

Mark A. Cappelli§
Stanford Plasma Physics Laboratory, Stanford, CA, 94305, USA

We present a simple, dynamic model for electron transport across the magnetic field of a Hall thruster and integrate this model into 2-D hybrid particle-in-cell simulations of a 72 mm diameter laboratory thruster operating at 400 W. The transport model is based on the assumption that the primary means of electron energy dissipation is the turbulent eddy cascade in the electron fluid to smaller scales. Implementing the model into 2-D hybrid simulations is relatively straightforward and leverages the existing framework for solving the electron fluid equations. We find that the model captures the strong axial variation in the mobility seen in experiments. In particular, it predicts the existence of a strong transport barrier which anchors the region of plasma acceleration. The model also captures the time-averaged experimental discharge current and its fluctuations due to ionization instabilities. We observe quantitative agreement with recent laser induced fluorescence measurements of time-averaged xenon ion and neutral velocities along the channel centerline.

*PhD Candidate, Mechanical Engineering Department, cvyoung@stanford.edu.
†PhD Candidate, Mechanical Engineering Department, escha@stanford.edu
‡Professor, Mathematics and Physics Department, fernane@eckerdd.edu
§Professor, Mechanical Engineering Department, cap@stanford.edu

Nomenclature

ϵ	= mean turbulent energy dissipation rate per unit mass (J/kg)
μ	= cross field mobility (m^2/s·V)
μ_{eff}	= effective cross field mobility (m^2/s·V)
ν_{eff}	= effective electron scattering rate (s^{-1})
ν_{turb}	= turbulent viscosity (m^2/s)
ρ_e	= electron Larmor radius (m)
ω_{ce}	= electron cyclotron frequency (rad/s)
$\vec{B}$	= magnetic field (vector) (T)
B	= magnetic field (magnitude) (T)
c_e	= mean electron speed (m/s)
$\vec{E}$	= electric field (vector) (V/m)
e	= fundamental charge (C)
$\vec{J}_{\text{e}}$	= electron current density (A/m^3)
K	= scaling constant for turbulent viscosity
ℓ	= characteristic turbulent eddy length scale
m_e	= electron mass (kg)
n_e	= electron density (m^{-3})
R	= radial thruster coordinate (m)
r	= radial thruster coordinate (m)
T_e	= electron temperature (eV)
u	= turbulent eddy velocity variation (relative to mean flow)
Z	= axial thruster coordinate (m)
z	= axial thruster coordinate (m)
LIF	= laser induced fluorescence
PIC	= particle-in-cell

I. Introduction

Hall thruster simulations have long sought to reproduce measurable characteristics of real devices to further our understanding of the complex physical processes governing cross-field electron transport, transient plasma fluctuations, and overall performance. Two-dimensional (2-D) hybrid particle-in-cell (PIC) simulations[1–4] strike a balance between computational effort and resolving realistic particle dynamics by treating electrons as a fluid and the heavy species (ions and neutrals) as discrete particles. In typical 2-D hybrid simulations, the domain comprises the radial-axial plane (defined by the magnetic and electric field vectors, respectively) in the channel and plume of a Hall thruster (see Fig. 1a).

Since this geometry does not resolve azimuthal fluctuations that are believed to drive cross-field transport of electrons, the electron mobility (and hence diffusion and thermal conductivity) must be modeled. Bohm diffusion was used in early hybrid codes, but the resulting discharge characteristics and performance exhibited poor agreement with experiments. Use of 2-D hybrid simulations was somewhat validated when an experimentally measured electron mobility was introduced.[5] This measured mobility contained a strong transport barrier that approached classical values near the exit of the channel, and climbed to anomalous values moving axially down- and upstream.[6] Computed discharge properties, including the axial variation in plasma density, temperature, potential, and ion velocity agreed reasonably well with experiments.[5] These results led to more refined models of electron transport, including one that assumed that shear in the electron fluid due to strong axial variations in the azimuthal electron drift near the channel exit plays a role in suppressing the growth of instabilities that would otherwise generate strong transport.[7] Ad-hoc models have also been used, some of which are based around the presence of a strong localized transport barrier,[8] and others that assume electron conductivity primarily via wall collisions inside the thruster and Bohm-scaled transport outside.[9,10] All such ad-hoc models must use several adjustable parameters to match the predicted plasma behavior with experimental measurements. A thorough review of the various transport models used in Hall thruster simulations appears in Ref. 11.

Despite the potential of the shear model presented in Ref. 7, it too has several unknown parameters that can potentially vary from one thruster to another. There remains, therefore, opportunities to improve the transportability of simulations between thrusters, or to other operating conditions and propellants, if a relatively simple, more universal description of the electron transport can be found. Recently, we proposed an isentropic model for the electron flow that inadequately captured thruster behavior over a broad range of conditions.[12] The isentropic model used an entropy conservation equation to close the set of electron fluid equations and solve for the electron mobility directly. This model was extended with a description of entropy production, but it too required ad-hoc parameterization in the entropy source term that we seek to avoid.[13,14]

The model described here continues our effort to derive a simple expression for the electron mobility that is robust, captures relevant physics, and is easily integrated into 2-D hybrid simulations. It is inspired by the approach described in Refs. 13 and 14, using the second law of thermodynamics to close the system of electron fluid equations. The model assumes that the primary means of electron energy dissipation is the turbulent eddy cascade in the electron fluid to smaller scales. As described below, the energy dissipation model produces the expected transport barrier seen in many Hall thrusters. It also favorably reproduces current-voltage trends and plasma properties (plasma temperature, electron density, and time-averaged ion velocities) of a legacy thruster whose electron transport is well characterized,[5] while a simpler Bohm transport approach performs poorly.

In this paper, we introduce the theory behind the dynamic turbulent dissipation model and detail its implementation in a 2-D radial-axial hybrid simulation of Stanford's 72 mm diameter, "Z70" laboratory Hall thruster. The calculated electron mobility is allowed to vary in time, and we begin by comparing predicted time-averaged results against recent laser induced fluorescence (LIF) neutral and ion velocity measurements of the thruster plume.[15,16] Our time-resolved LIF ion velocity measurements show strong fluctuations in ion velocity over the course of the 23 kHz breathing mode cycle, however, and reproducing time variation in the measured Hall thruster quantities of interest throughout the oscillation cycle — along with the average value — represents the next benchmark for improving simulations towards a predictive capability for aiding thruster design. These time-resolved measurements will be compared against results from this simulation in a future publication.

II. Turbulent Electron Transport Model

The plasma inside the channel and into the near-field plume of Hall discharge thrusters is very turbulent. Early literature described the presence of a plethora of fluctuations spanning a wide spectrum of frequencies.[17] Studies of plasma density fluctuations inside a thruster discharge channel using probes[18] show a characteristic energy spectrum over wavenumber scales typical of a turbulent flow: an energy production regime exists at large scales, followed by an inertial regime at wavelengths comparable to the electron Larmor radius that appears to decay into a power law regime characteristic of dissipation at a scale comparable to the electron mean free path. The intensity of this plasma turbulence seems to correlate with the measured cross-field mobility, perhaps suggesting a causal relationship.[6] Experiments have also reported fluctuations at very high frequencies,[19,20] particularly outside of the thruster channel. It is well known that correlated fluctuations between plasma density and potential can give rise to cross-field current exceeding that predicted classically. Near the exit plane, where electrons drift azimuthally and ions drift axially, the system can support well-known streaming instabilities,[21] resistive instabilities,[22,23] and Rayleigh-Taylor type instabilities.[24] Further upstream into the channel and downstream into the plume, there are strong gradients in plasma density, temperature, and magnetic fields. These gradients can also render drift waves to be unstable.[25,26] Such instabilities, which fall under the inertial range of wavelength scales, were first predicted to be relevant to Hall thruster operation several decades ago.[27]

As mentioned above, most plasma thruster simulations that span the thruster channel (and beyond up to the cathode plane) do not resolve either the length scales or the spatial dimensions (e.g., the azimuthal direction) necessary for adequately describing the fluctuations that may be important drivers of electron transport. As a recourse, one must resort to using a transport model, and deriving transport models built around the presence of turbulent fluctuations is a challenging task. As in the development of transport models for neutral fluid turbulence, a zero-equation model can be a useful first approach.[28] A zero-equation model attempts to describe the turbulent viscosity and energy dissipation rate with dimensionally-inspired algebraic equations, without resorting to solutions of differential equations for the turbulent kinetic energy and its rate of dissipation.

The zero-equation model that we develop here begins with the usual scaling for the turbulent energy cascade, where the mean rate of turbulent energy dissipation (per unit mass), ϵ, is expressed in terms of the turbulent viscosity, ν_{turb}:[29]

$$\epsilon = \nu_{\mathrm{turb}} \left(\frac{u}{\ell}\right)^2 \tag{1}$$

Here, ℓ is the characteristic length scale, and u is the velocity variation (relative to the mean flow) of the turbulent eddies. The term in parenthesis represents the spatial variation in the turbulent velocity field, indicative of the large eddy turnover time. The turbulence is expected to be electrostatic in nature, in which fluctuations in plasma density and mean velocities are accompanied by variations in plasma potential. In discharge plasmas, these fluctuations can be strongly correlated and can give rise to excursions in particle fluxes that contribute to (anomalous) current beyond that expected from classical mechanisms (scattering collisions between particles following particle drifts driven only by local electric and magnetic fields). The electrostatic energy associated with these fluctuations may constitute a significant fraction of the system total. We assume that electrons migrating from the cathode to the anode will eventually convert their kinetic energy into electrostatic fluctuations. This same class of electrons may also scatter from these fluctuations, depleting their kinetic energy and converting it to thermal energy. In essence, this dissipative mechanism is analogous to electron Joule heating. In our modeling, we will assume that this process is the dominant mechanism for electron thermalization.

Proceeding with a model for the dissipation rate ϵ requires expressions for ν_{turb} and the eddy turnover rate, u/ℓ. The scaling of ν_{turb} follows the early work of Prandtl,[30] which is based on an analogy with kinetic theory. We assume that the characteristic scale of the largest eddies is the local electron Larmor radius, ρ_e, which is about 1 mm in the channel of a Hall thruster close to the peak magnetic field (B = 100 G, T_{e} = 20 eV). This is consistent with the scale of the fluctuations in 2-D current distributions seen in the PIC simulations of Adam et al.[31] We shall also assume that the velocity scale for eddy transport is the mean electron speed, c_{e}, which represents an upper limit for the transport of high frequency fluctuations. We therefore express the turbulent viscosity as:

$$\nu_{\mathrm{turb}} = K \rho_{\mathrm{e}} c_{\mathrm{e}} \tag{2}$$

where K is a constant that will be derived from experiments. Ideally, the constant K will be transportable to similar Hall discharges, perhaps of differing geometries and operating on different propellants. This constant is the only parameter that must be specified, and we expect it to be of order unity.

Rather than attempting to scale the eddy turnover rate, we shall assume that electrons are scattered from the fluctuations at a rate equal to u/ℓ. This effective electron scattering rate, $\nu_{\rm eff}$, is related to the electron cyclotron frequency, $\omega_{\rm ce} = c_{\rm e}/\rho_{\rm e}$, and the effective cross field mobility, $\mu_{\rm eff}$, in the limit of weak collisionality ($\nu_{\rm turb}/\omega_{\rm ce} \ll 1$):

$$\mu_{\rm eff} = \frac{\nu_{\rm eff}}{\omega_{\rm ce} B}. \tag{3}$$

Equations (1)–(3) are combined, with $\nu_{\rm eff} = u/\ell$, to form a new expression for the turbulent energy dissipation rate:

$$\epsilon = K c_{\rm e}^2 \omega_{\rm ce} B^2 \mu_{\rm eff}^2. \tag{4}$$

Equation (4), when multiplied by the electron mass density ($n_{\rm e} m_{\rm e}$), is taken to represent Joule heating, as discussed above. Making this equivalence and solving for effective mobility yields:

$$\mu_{\rm eff} = \left(\frac{\vec{J}_{\rm e} \cdot \vec{E}}{K n_{\rm e} e c_{\rm e}^2 B^3} \right)^{1/2} \tag{5}$$

where e is the fundamental charge. The electron current densities, $\vec{J}_{\rm e}$, and electric field, $\vec{E}$, (along with the other necessary plasma parameters) are computed directly in the 2-D hybrid simulation, making implementation of this model relatively straightforward. The simulations are discussed briefly in the next section.

III. Hybrid Simulation

The turbulent dissipation model for cross-field mobility is implemented in a 2-D hybrid radial-axial Hall thruster simulation that is described in further detail elsewhere[2,5] and is similar to those developed by others.[1,3,4] As shown in Fig. 1a, the hybrid simulation models the plasma in a plane perpendicular to the azimuthal direction in the thruster channel and just beyond the exit plane to where the cathode intersects the last magnetic flux surface (Fig. 1c, cathode not shown). The heavy species constituents (xenon neutrals and ions) are treated as discrete superparticles, representing a group of real particles. Ions are accelerated by the electric field using a particle-in-cell (PIC) approach, and electron impact ionization and recombination at the walls is treated using Monte Carlo methods. Assuming quasi-neutrality, the PIC component of the simulation computes the ion velocity and the plasma density, which is mapped onto the grid used to solve the fluid equations (continuity, radial and axial momentum, and energy) for the electron velocity, electric potential, and electron temperature. Time steps of 1 ns and 25 ns are used for advancing the electrons and heavy particles, respectively.

Here, we build on the confidence developed in these simulations over several years to test how well the simple zero-equation turbulence model for the electron mobility reproduces reasonable values for the plasma properties. The Z70[15] is a SPT-type Hall thruster developed at Stanford that has a similar magnetic topology and geometry to commercial Hall thrusters. It has a channel length of 2.3 cm, an outer diameter of 7.2 cm, and an inner diameter of 4.2 cm. The computational grid for the PIC portion of the code is illustrated in Fig. 1b. The imposed static magnetic field, B, is shown in Fig. 1c, simulated using a commercial finite element solver.[32] The magnetic topology is also shown in Fig. 1c; the electron fluid equations are solved in 1-D on 800 magnetic contours assuming isothermal electrons (infinite conductivity) in the directions parallel to the imposed field. We run the thruster at a discharge voltage of 240 V and a mass flow rate of 2 mg/s (xenon). Under these conditions, the experimental discharge current (Fig. 2a) fluctuates at $\sim$ 23 kHz quasi-coherently with a mean of about 1.7 A. The fundamental breathing mode frequency and several harmonics are visible in an FFT of the current trace.

IV. Results

Using the turbulent transport model given by Eqn. 5, the 2-D hybrid simulation runs stably for many tens of breathing mode cycles. A weighting constant of $K = 2.5$ is used in the simulation to match the

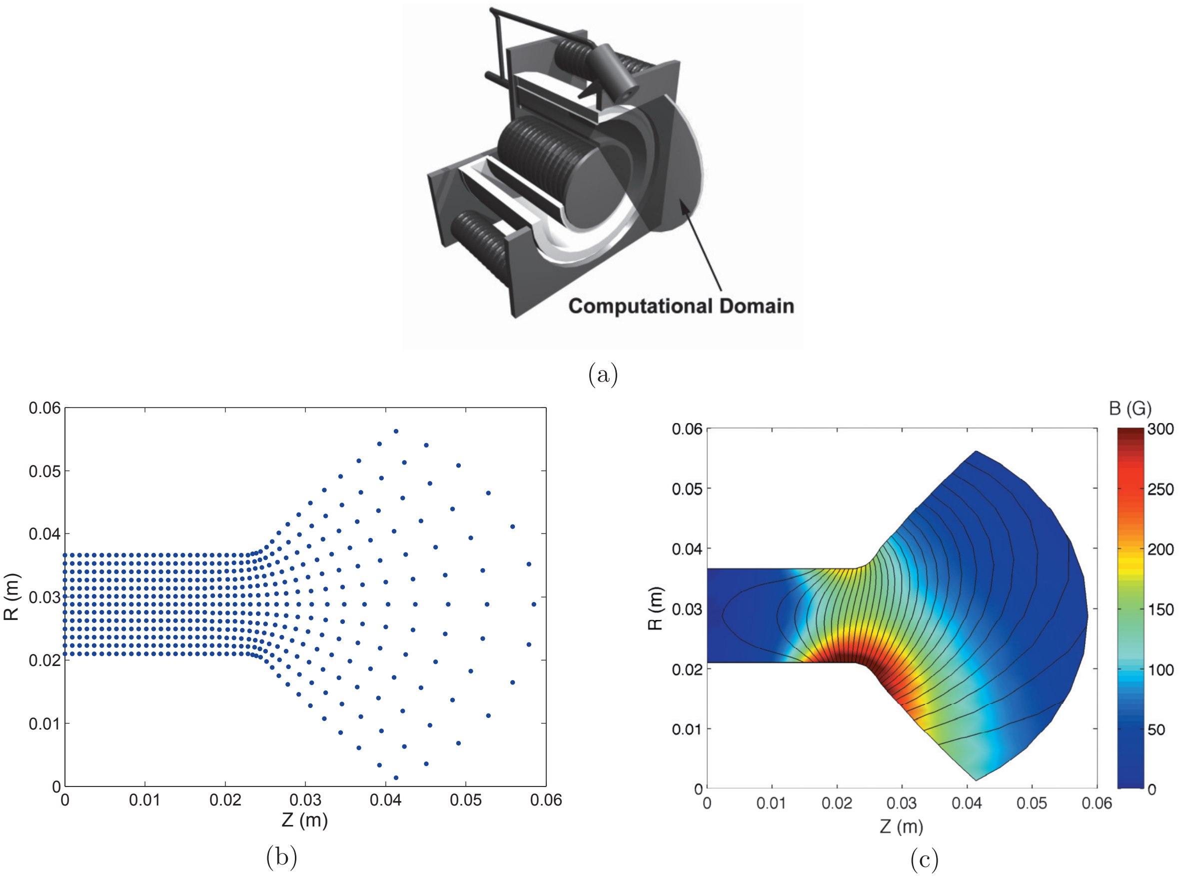

Figure 1. (a) 2-D radial-axial (R-Z) plane for the hybrid PIC Hall thruster simulation. (b) Computational mesh for the PIC solver. (c) Total magnetic field strength (G) in the domain, with magnetic contours overlaid.

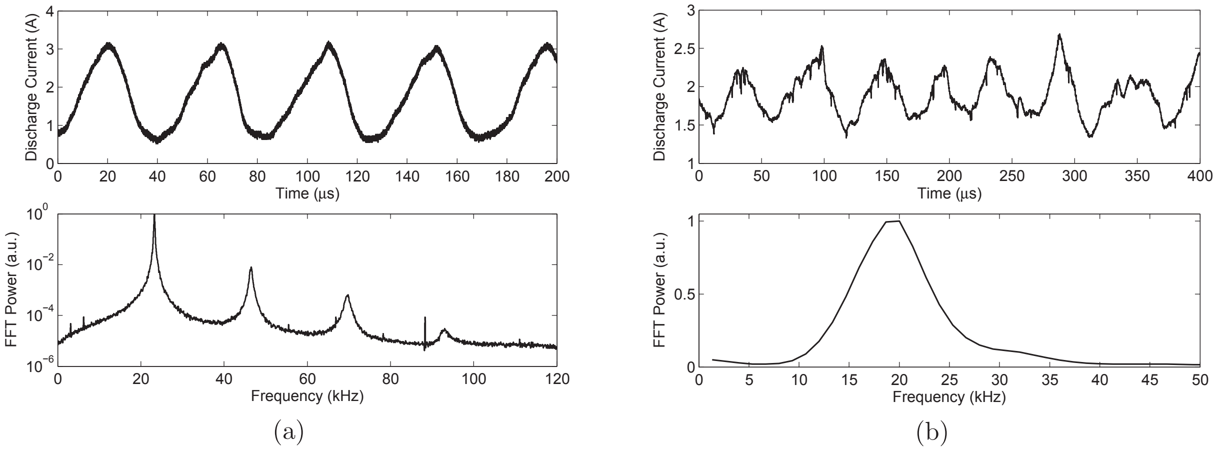

Figure 2. Thruster discharge current and (smoothed) FFT profiles measured from (a) experiments, and (b) the hybrid PIC simulation. Fewer oscillation periods are captured in the simulation, leading to a broader frequency spectrum in the FFT.

time-averaged discharge current measured in the Z70 (1.7 A). The dynamical calculation of the electron mobility is under-relaxed for improved stability of the simulation. By this we mean that at every electron fluid time step, approximately half of the instantaneously computed mobility is averaged with half of that computed in the previous time step.

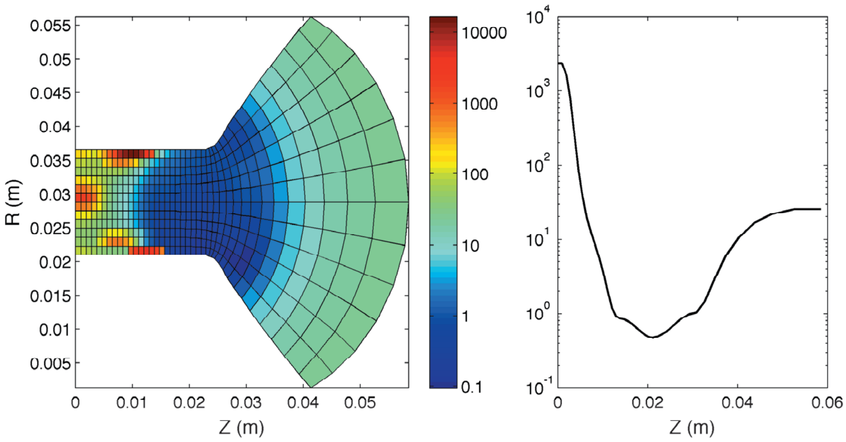

Figure 3. Time-averaged profiles of the electron mobility ($\mathbf{m^2/s{\cdot}V}$) calculated with the turbulent dissipation model over the full 2-D domain (left), and along the channel centerline, $\boldsymbol{R = 2.9}$ cm (right).

The predicted discharge current is shown in Fig. 2b. Although not as coherent as those seen in experiments, the breathing mode oscillations do seem to capture strong excursions in discharge current ($\sim \pm 0.6$ A) about the mean (1.8 A). Note that fewer oscillation periods are incorporated into the calculation of the current FFT, leading to much less frequency resolution and a broader feature when compared with experimental measurements. Averaging the calculated electron mobility over time throughout the domain yields the plots presented in Fig. 3. The left panel shows the average mobility over the entire computational domain, whereas the right panel shows the calculated average mobility along the channel centerline ($R = 2.9$ cm). The time-averaged mobility captures the presence of a strong transport barrier in this region that falls steeply upstream of the exit plane. Note that near the anode, the mobility has been clamped to that predicted classically to avoid unphysically large mobilities stemming from magnetic field values that are nearly zero. Moving downstream into the plume, the transport barrier rises more gradually before plateauing at about 26 $m^2/s{\cdot}V$. We note that in the Bohm limit, the mobility $\mu \propto 1/16B$. In this near-field region, with $B \approx 10^{-2}$ T, $\mu \approx 6$ $m^2/s{\cdot}V$. Therefore, the turbulence model predicts near-Bohm values of transport in this region of the flow.

Computed time-averaged values of important plasma properties along the channel centerline are reported in Fig. 4, including the plasma potential, axial ion velocity, plasma density, electron temperature, neutral velocity, and neutral number density. There exists a strong electric field reversal near the anode (plasma potential "hump" greater than the 240 V applied to the anode), produced largely by strong plasma density gradients that drive excess electrons towards the anode. The ion velocity increases rapidly near the exit of the channel ($Z = 2.3$ cm) and beyond, indicating a largely external acceleration process. Within ~ 1 cm from the anode, ions reverse direction and stream towards the anode — consistent with the observed electric field reversal. Neutral xenon accelerates monotonically in the axial direction. This apparent acceleration is attributed to the preferred ionization of slow neutrals, which spend a greater residence time within the channel. The solid symbols in the velocity figures represent experimental laser induced fluorescence data obtained for this thruster.[16] The measured ion acceleration profile is captured by the simulation, although the code places the accelerating potential drop slightly further upstream than seen experimentally. The simulation also predicts a slightly higher terminal neutral velocity downstream of the ionization zone.

Fig. 5 depicts 2-D colormaps of the same computed time-average plasma properties. Much of the structure in these plots follows that of the centerline trends seen in Fig. 4. The plasma density is maximum just upstream of the exit plane, and trails off near the channel walls as a result of the imposed wall loss conditions. The neutral density and velocity in the anode region is higher on near the center of the channel due to centerline injection of neutrals at the anode.

Finally, in Fig. 6 we compare time-averaged ion velocity distribution functions (IVDFs) at four locations in the plume along the channel centerline. Solid lines depict IVDFs calculated using the hybrid simulation, and dotted lines show those measured by time-averaged LIF.[16] Mass-weighted average velocities obtained from calculated VDFs such as these are what appear in Figs. 4 and 5, while the most-probable (peak)

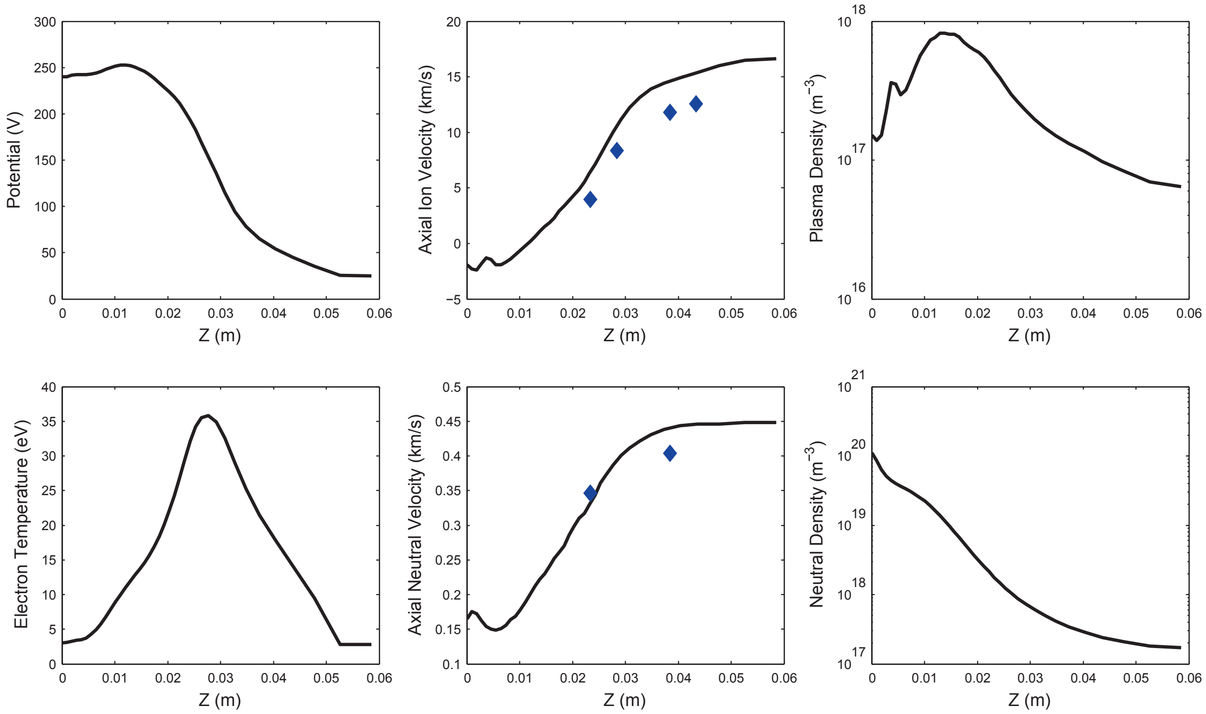

Figure 4. Calculated time-averaged plasma properties along the channel centerline, $R = 2.9$ cm. The symbols (♦) indicate data from time-averaged laser induced fluorescence measurements of the Z70 plume.[16]

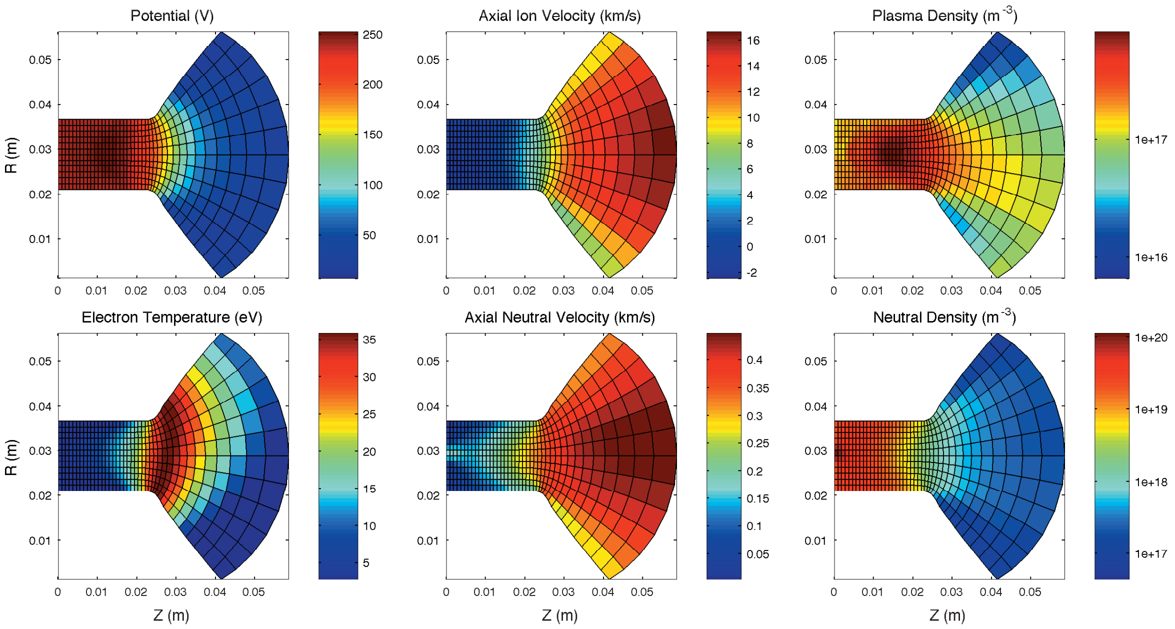

Figure 5. Calculated time-averaged plasma properties over the entire 2-D simulation domain. Data from the centerline at $R = 2.9$ appears in Fig. 4.

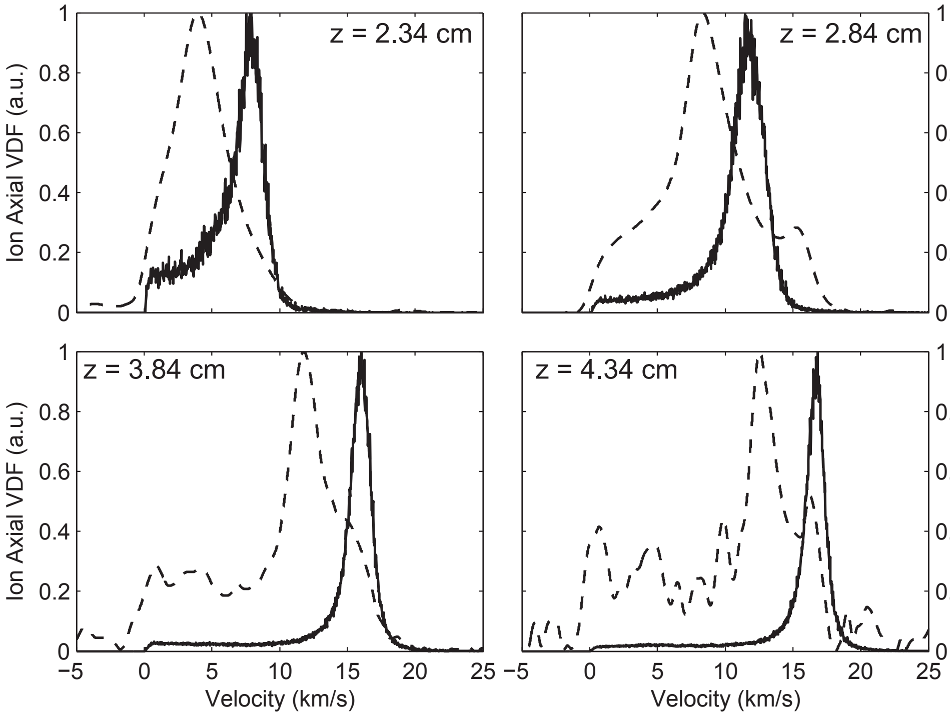

Figure 6. Axial time-averaged ion velocity distribution functions measured (dotted lines) and calculated (solid lines) at four locations in the Z70 plume along the channel centerline.

velocity from the experimental traces are recorded on those figures. As mentioned previously, the code predicts ion acceleration to occur farther upstream than seen experimentally. However, the widths of the main feature (velocity spread) in each case are comparable. As ion density decreases farther into the plume, the measured traces experience more noise due to fewer fluorescence signal photons relative to the bright background emission. At $z = 4.34$ cm, evidence of a low velocity ion population appears in the measured IVDF, the time-dependent behavior of which is detailed in other publications.[15,16] As this paper focuses on time averaged behavior, it is sufficient to note that the hybrid simulation fails to reproduce this effect. This would be the case if low velocity population originates from the opposite side of the channel (an effect of the annular geometry), as the simulation does not account for other regions of the annular channel outside the computational domain. Analysis of the measured and simulated time variation of the IVDFs throughout the breathing mode cycle will be conducted in a future publication.

V. Summary and Future Work

This paper describes a dynamic model for cross-field electron transport in hybrid particle-in-cell simulations of Hall thrusters. The model assumes that the primary means of electron energy dissipation is the turbulent eddy cascade to smaller length scales and leverages a simple zero-equation approach to describe the conversion of electron kinetic energy into Joule heating of the plasma. Through simple scaling relations, we obtain an expression for effective mobility that reacts to local evolving plasma conditions and is easily incorporated into an existing hybrid PIC framework.

Simulations of the Stanford Plasma Physics Laboratory Z70 Hall thruster operating on xenon at 400 W are conducted and compared against time-averaged laser induced fluorescence measurements of axial neutral and ion velocities. With some discrepancies, the model achieves quantitative agreement with measured plasma parameters, including average discharge current. ~ 20 kHz breathing mode fluctuations are observed both experimentally and in the simulation. The turbulent dissipation model successfully produces expected phenomena, including a strong barrier to cross-field electron transport near the exit plane and a gradient-driven electric field reversal near the anode. The ion acceleration is predicted to occur farther upstream than seen experimentally, although the general profile is recovered. Time-averaged ion velocity distribution functions in the plume show differing peak locations but similar widths in velocity space.

Future studies will examine the time-dependent behavior of the hybrid PIC simulation on the time scale of breathing mode oscillations and compare further with time-resolved laser induced fluorescence measurements of ion and neutral species. The transportability of the turbulent transport model will be assessed using simulations of different thrusters, and further comparisons with existing transport models will verify its accuracy at recovering known thruster parameters. We hope that such a dynamic mobility model will soon enable hybrid simulations to produce close agreement with real devices varying with time, not just in time-average.

Acknowledgments

This work is sponsored by the U.S. Air Force Office of Scientific Research with Dr. M. Birkan as program manager. C.Y. acknowledges support from the DOE NSSA Stewardship Science Graduate Fellowship under contract DE-FC52-08NA28752 and the Stanford Graduate Fellowship.

References

[1]Fife, J. M., *Two-dimensional hybrid particle-in-cell modeling of Hall thrusters*, Ph.D. thesis, Massachusetts Institute of Technology, 1995.

[2]Fernandez, E., Cappelli, M. A., and Mahesh, K., "2D simulations of Hall thrusters," *Ctr annual research briefs*, 1998, pp. 81–90.

[3]Boeuf, J. P. and Garrigues, L., "Low frequency oscillations in a stationary plasma thruster," *Journal of Applied Physics*, Vol. 84, No. 7, 1998, pp. 3541–3554.

[4]Koo, J. W. and Boyd, I. D., "Computational model of a Hall thruster," *Computer physics communications*, Vol. 164, No. 1, 2004, pp. 442–447.

[5]Scharfe, M. K., Gascon, N., Cappelli, M. A., and Fernandez, E., "Comparison of hybrid Hall thruster model to experimental measurements," *Physics of Plasmas (1994-present)*, Vol. 13, No. 8, 2006, pp. 083505.

[6]Meezan, N. B., Hargus Jr, W. A., and Cappelli, M. A., "Anomalous electron mobility in a coaxial Hall discharge plasma," *Physical Review E*, Vol. 63, No. 2, 2001, pp. 026410.

[7]Scharfe, M. K., Thomas, C. A., Scharfe, D. B., Gascon, N., Cappelli, M. A., and Fernandez, E., "Shear-based model for electron transport in hybrid Hall thruster simulations," *Plasma Science, IEEE Transactions on*, Vol. 36, No. 5, 2008, pp. 2058–2068.

[8]Cheng, S. and Martinez-Sanchez, M., "Hybrid particle-in-cell erosion modeling of two Hall thrusters," *Journal of Propulsion and Power*, Vol. 24, No. 5, 2008, pp. 987–998.

[9]Garrigues, L., Pérez-Luna, J., Lo, J., Hagelaar, G. J. M., Boeuf, J. P., and Mazouffre, S., "Empirical electron cross-field mobility in a Hall effect thruster," *Applied Physics Letters*, Vol. 95, No. 14, 2009, pp. 141501–141501.

[10]Koo, J. W. and Boyd, I. D., "Modeling of anomalous electron mobility in Hall thrusters," *Physics of Plasmas (1994-present)*, Vol. 13, No. 3, 2006, pp. 033501.

[11]Hofer, R. R., Katz, I., Mikellides, I. G., Goebel, D. M., Jameson, K. K., Sullivan, R. M., and Johnson, L. K., "Efficacy of Electron Mobility Models in Hybrid-PIC Hall Thruster Simulations," *AIAA Paper*, Vol. 4924, 2008, pp. 2008.

[12]Knoll, A. K. and Cappelli, M. A., "A simple isentropic model of electron transport in Hall thrusters," *J. Phys. D: Appl. Phys*, Vol. 41, No. 162003, 2008, pp. 162003.

[13]Cappelli, M. A., Cha, E., and Fernandez, E., "Entropy closure model for transport in Hall thruster simulations," *Proc. 33rd Int. Electr. Propuls. Conf*, 2013, pp. 2013–088.

[14]Cha, E., Cappelli, M. A., and Fernandez, E., "Implementation of an Entropy Closure Model for 2-D Hybrid Hall Thruster Simulations," 2015.

[15]Young, C. V., Lucca Fabris, A., and Cappelli, M. A., "Ion dynamics in an $E \times B$ Hall plasma accelerator," *Applied Physics Letters*, Vol. 106, No. 4, 2015, pp. 044102.

[16]Young, C. V., Lucca Fabris, A., and Cappelli, M. A., "Time-Synchronized Laser Induced Fluorescence Measurement of Xenon Ion and Neutral Dynamics in a 350 W Hall Thruster," *Proceedings of the 34th Internationl Electric Propulsion Conference*, No. IEPC-2015-437, Hyogo-Kobe, Japan, July 4-10 2015.

[17]Choueiri, E. Y., "Plasma oscillations in Hall thrusters," *Physics of Plasmas (1994-present)*, Vol. 8, No. 4, 2001, pp. 1411–1426.

[18]Gascon, N. and Cappelli, M. A., "Plasma instabilities in the ionization regime of a Hall thruster," *Proceedings of the 39th Joint Propulsion Conference (American Institute of Aeronautics and Astronautics, 2003), AIAA-2003-4857*, 2003.

[19]Lazurenko, A., Albarede, L., and Bouchoule, A., "Physical characterization of high-frequency instabilities in Hall thrusters," *Physics of Plasmas (1994-present)*, Vol. 13, No. 8, 2006, pp. 083503.

[20]Tsikata, S., Lemoine, N., Pisarev, V., and Grésillon, D. M., "Dispersion relations of electron density fluctuations in a Hall thruster plasma, observed by collective light scattering," *Physics of Plasmas (1994-present)*, Vol. 16, No. 3, 2009, pp. 033506.

[21]Baranov, V. I., Nazarenko, Y. S., Petrosov, V. A., Vasin, A. I., and Yashnov, Y. M., "Theory of oscillations and conductivity for Hall thruster," *Proc. 32nd AIAA Joint Propulsion Conference*, 1996.

[22]Litvak, A. A. and Fisch, N. J., "Resistive instabilities in Hall current plasma discharge," *Physics of Plasmas (1994-present)*, Vol. 8, No. 2, 2001, pp. 648–651.

[23]Fernandez, E., Scharfe, M. K., Thomas, C. A., Gascon, N., and Cappelli, M. A., "Growth of resistive instabilities in $E \times B$ plasma discharge simulations," *Physics of Plasmas (1994-present)*, Vol. 15, No. 1, 2008, pp. 012102.

[24]Litvak, A. A. and Fisch, N. J., "Rayleigh instability in Hall thrusters," *Physics of Plasmas (1994-present)*, Vol. 11, No. 4, 2004, pp. 1379–1383.

[25]Kapulkin, A. and Guelman, M. M., "Low-Frequency Instability in Near-Anode Region of Hall Thruster," *Plasma Science, IEEE Transactions on*, Vol. 36, No. 5, 2008, pp. 2082–2087.

[26]Frias, W., Smolyakov, A. I., Kaganovich, I. D., and Raitses, Y., "Long wavelength gradient drift instability in Hall plasma devices. I. Fluid theory," *Physics of Plasmas*, Vol. 19, No. 7, 2012, pp. 072112.

[27]Morozov, A. I., Esipchuk, Y. V., Kapulkin, A. M., Nevrovskii, V. A., and Smirnov, V. A., "Azimuthally asymmetric modes and anomalous conductivity in closed electron drift accelerators," *Soviet Physics Technical Physics*, Vol. 18, 1973, pp. 615.

[28]Baldwin, B. S. and Lomax, H., *Thin layer approximation and algebraic model for separated turbulent flows*, Vol. 257, American Institute of Aeronautics and Astronautics, 1978.

[29]Landau, L. D. and Lifshitz, E. M., "Fluid mechanics, vol. 6," *Course of Theoretical Physics*, 1987, pp. 116–121.

[30]Doshi, M. R. and Gill, W. N., "A note on the mixing length theory of turbulent flow," *AIChE Journal*, Vol. 16, No. 5, 1970, pp. 885–888.

[31]Adam, J. C., Boeuf, J. P., Dubuit, N., Dudeck, M., Garrigues, L., Gresillon, D., Heron, A., Hagelaar, G. J. M., Kulaev, V., Lemoine, N., and others, "Physics, simulation and diagnostics of Hall effect thrusters," *Plasma Physics and Controlled Fusion*, Vol. 50, No. 12, 2008, pp. 124041.

[32]Meeker, D., "Finite Element Method Magnetics," http://www.femm.info/wiki/HomePage, Jun 2011.